

# A FILTER-DESIGN METHOD BASED ON ELECTRICAL-LINE GRIDS FOR SINGLE-PHASE TOPOLOGIES USING BPL

Ing. PhD. Octavio J. Salcedo Parra, Ing Rafael Enrique Balaguera Hernández, Ing. Brayan S. Reyes Daza \*

Intelligent Internet Research Group

Universidad Distrital "Francisco Jose de Caldas" Facultad Ingeniería

Bogotá DC, Colombia

osalcedo@udistrital.edu.co, rbalaguera@pedagogica.edu.co, bsreyesd@correo.udistrital.edu.co

**Abstract:** *The present work aims to determine a method for modeling and designing different types of filters that exist between nodes in a single phase topology with BPL technology for housing. The filter design objectives are to control the spectral power density, with the effect of the BPL transmission power is optimized and significant offset voltage variations that occur in the connection and disconnection of electric charges, both effects are presented in a phase topology that is used as the communication channel. The results are reflected in the attenuation of electromagnetic compatibility (noise, attenuation, distortion, and coupling) relevant variables that cause problems on the communication channel of a system with BPL technology.*

**Keywords:** communication channel, filter, power spectral density, single-phase topology.

## INTRODUCTION

The possibility of using electrical energy grids as a channel for communication-signal transmissions involves introducing a conceptual and technological framework that has evolved in its terminology but still addresses the very same issues. Initially, these technological ideas were referred to as PLT (*Power Line Telecommunication*), occasionally also called PLC (*Power Line Communication*); at present, the term to be used is BPL (*Broadband over Power Line*), [2]-[4].

There are various restrictions associated to electrical grids when they are used as a channel for the transmission of communication signals [5]-[16]-[17], namely:

- a. Electromagnetic compatibility problems (e.g. noise, attenuation, distortion and line coupling) derived from line design, which is originally intended for electrical power transmission only.
- b. Electrical load connecting and disconnecting events, which cause significant voltage variations that affect the topology of the electrical lines that serve as communication channel.
- c. Configuration issues: there are aerial as well as underground grids.
- d. Operation voltage levels and user grid topologies: there are variations between 110 V<sub>ac</sub> and 1 KVac depending on the application and purpose (either residential, commercial or industrial). Additionally, in terms of topology design, the following configurations are

possible: single-phase, two-phase and three-phase including ground connections and protection circuit synchronization.

Depending on the type of restriction and/or combination of restrictions, a different analysis should be conducted to meet the required BPL condition [6]. In this particular study, an electrical-line grid-based method is established in order to design suitable filters to be placed in between nodes derived from a single-phase topology that serves as communication channel, starting from a set of extracted transfer functions.

## METHODOLOGY

When applying an observation-based methodology to look at existing research results it is possible to determine the elements that lead to the intended method. Prior analysis leads to the following:

- a. Convenient geometry and configuration of a single-phase topology, which is modeled as a distributed parameter transmission line (with and without load). For various types of AWG conductors and loads it is possible to determine transmission line parameters by applying characteristic electromagnetic relations.
- b. The elements that constitute the transmission line model, which find their place within a quadripole model. The transmission parameters in question [3]-[13] allow characterization of each transmission-line element in a matrix form.
- c. Finding the transmission matrix; this allows proper control of frequency variations as well as length variations over the transmission line model.

## 1. PRELIMINARY DEVELOPMENT OF THE METHOD

In order to represent a distributed-parameter transmission line for a single-phase topology (which corresponds to the two-conductor model), it is necessary to use electromagnetic relations that allow modeling each of the line's constituent elements from a geometric perspective; this process is called parameterization. The representation of a transmission line with no load is shown in Figure 1.

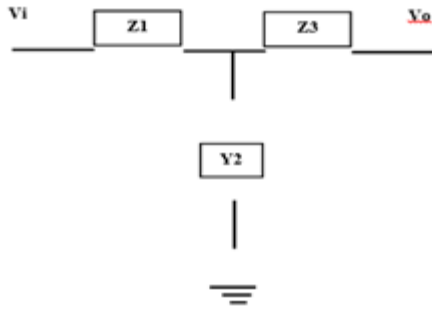


Figure 1: Transmission line with no load

Z1 and Z2 correspond to the input and output impedances, respectively, and Y2 represents the transmission line admittance.

The material considered as dielectric (material that covers the conductor) was chosen to be an intermediate compound between polystyrene and asbestos, thus its relative permittivity is  $\epsilon_r = 3.45$ . As a conductor, copper was chosen, thus relative permeability is  $\mu_r = 1$ . The particular conductor to be analyzed corresponds to a copper 12-AWG wire within a PVC pipeline – 1/2" galvanic metallic conduit [5]. In this case, the associated absolute values of permittivity and permeability are as follows:

$\epsilon = \epsilon_0 \cdot \epsilon_r$	$\mu = \mu_0 \cdot \mu_r$
3,05469E-11	1,25664E-06

(1)

## PARAMETER DESCRIPTION

### 1.1. Skin depth

Any current density or electrical field intensity falls towards the center of solid conductors. Electromagnetic energy does not travel at the core of conductors; instead, energy flows over the surface of conductors, thus a conductor serves to guide electrical waves. The currents that occur on the surface of conductors propagate towards the inner conductor and are perpendicular to current density; in doing so, such current is also attenuated by resistive losses. In some books, this phenomenon is referred to as skin effect and is denoted by  $\delta$ ; similarly, resistive losses are denoted by  $\tan\delta$ .

Equation 2 shows the variation of this parameter as a function of frequency (f), material permeability ( $\mu$ ) and material conductivity ( $\sigma_c$ ). Table 4 shows the values of these parameters for various types of conducting materials at different operation frequencies, namely 60 Hz, 1.8 MHz and 30 MHz.

$$\delta = \frac{1}{\sqrt{\pi \cdot f \cdot \mu \cdot \sigma_c}}; (mts) \quad (2)$$

Table 1: The values of the parameters

CALIBRE (AWG)	f = 60 Hz		f = 1.8 MHz		f = 30 MHz	
	PROFUNDIDAD DE LA PELÍCULA $\delta = 1/\sqrt{\pi f \mu \sigma_c}$ (mts)	FACTORES PÉRDIDAS $\tan\delta$	$\delta$ (mts)	$\tan\delta$	$\delta$	$\tan\delta$
6	3,91E-03	1,48E-04	4,92E-05	3,97E-07	1,20E-05	2,06E-07
8	3,91E-03	1,48E-04	4,92E-05	3,97E-07	1,20E-05	2,06E-07
10	3,91E-03	1,48E-04	4,92E-05	3,97E-07	1,20E-05	2,06E-07
12	3,91E-03	1,48E-04	4,92E-05	3,97E-07	1,20E-05	2,06E-07
14	3,91E-03	1,48E-04	4,92E-05	3,97E-07	1,20E-05	2,06E-07
16	4,03E-03	1,03E-04	3,48E-05	6,07E-07	9,53E-06	1,40E-07

Table 2: Skin depth and transmission losses are higher for low frequencies

CALIBRE (AWG)	DIÁMETRO=2R (mts)	de penetración (%)		
		f=60 Hz	f=1.8 MHz	f=30 MHz
6	0,004113357	68%	0,393%	0,0962%
8	0,003052598	73%	0,421%	0,1032%
10	0,002585401	77%	0,447%	0,1095%
12	0,002049085	81%	0,470%	0,1153%
14	0,001602372	85%	0,490%	0,1200%
16	0,001201489	62%	0,353%	0,0877%

In Table 2, it can be observed that skin depth and transmission losses are higher for low frequencies. For operation frequencies associated to BPL transmissions ranging from 1.8 MHz to 30 MHz, the communications signal should travel between the conductor's surface and the dielectric material, since there is very low skin depth for these frequencies.

### 1.2. Attenuation Constant, Phase Constant, Propagation Constant and Wave Propagation Speed.

When propagating through a conductor (wire or cable including the surrounding dielectric sleeve), an electrical signal changes its characteristics and transmission values (e.g. attenuation, phase, propagation, speed and wavelength) due to conductivity ( $\sigma_c$ ) and absolute permittivity- ( $\epsilon$ ) permeability- ( $\mu$ ) losses associated to different materials.

The factor that allows considering the attenuation over an electrical signal, when propagating in a particular direction through a lossy medium, is called attenuation constant ( $\alpha$ , nepers/m; Np/m). Similarly, the measurement of the signal's phase shift is called phase constant ( $\beta$ , radians/m; rad/m). The combination of  $\alpha$  and  $\beta$  yield a propagation complex constant ( $\gamma$ ).

$$\gamma = \alpha + j\beta \quad (3)$$

$$\gamma = j\omega \cdot \sqrt{\mu \cdot \epsilon} \cdot \sqrt{\left(1 - \frac{j\sigma}{\omega \epsilon}\right)} \quad (4)$$

The following tables provide a context by summarizing the values of the aforementioned constants for particular frequencies, namely 60 Hz, 1.8 MHz and 30 MHz.

**Table 3:** Values of the aforementioned constants for particular frequencies (3).

frecuencia: 1.8 MHz	REAL	IMA	NORMA	ÁNGULO
$(1 - (j\omega/\omega_c)) =$	1,000	-0,17	1,014	-9,53889
$\sqrt{(1 - (j\omega/\omega_c))} =$	0,994	1,003	1,00097	85,23456
$\gamma = j\omega \cdot \sqrt{(\mu \cdot \epsilon)} \cdot \sqrt{(1 - (j\omega/\omega_c))} =$	0,00586191	0,07031423	0,07056015	85,23456
$\alpha =$	0,00586191	Np/m		
$\beta =$	0,07031423	Rad/m		

**Table 4:** Values of the aforementioned constants for particular frequencies (4).

frecuencia: 30 MHz	REAL	IMA	NORMA	ÁNGULO
$(1 - (j\omega/\omega_c)) =$	1,000	-0,01	1,000	-0,57707
$\sqrt{(1 - (j\omega/\omega_c))} =$	0,995	1,000	1,00003	89,70143
$\gamma = j\omega \cdot \sqrt{(\mu \cdot \epsilon)} \cdot \sqrt{(1 - (j\omega/\omega_c))} =$	0,00588231	1,16787262	1,167887423	89,70143
$\alpha =$	0,00588231	Np/m		
$\beta =$	1,16787262	Rad/m		

Figures from Tables 3 and 4 indicate that attenuation constant  $\alpha$  is lower at low frequencies, in other words, electromagnetic fields suffer attenuations equivalent to a factor of  $e^{-1} = 0.3678$  every  $1/0.0001172 = 8532.42$  meters at 60 Hz, every  $1/0.00586191 = 170.59$  meters at 1.8 MHz and every  $1/0.00588231 = 170.001$  meters at 30 MHz. Phase constant  $\beta$  gradually increases as frequency increases. Similarly, propagation complex constant  $\gamma$  increases in magnitude and phase as frequency increases.

### 1.3. Primary parameters of a two-conductor transmission line

The context to analytically determine the primary parameters of a transmission line (that is associated to a single-phase household topology with BPL and is used as a telecommunications channel) corresponds to a PVC pipeline 1/2" galvanized metallic conduit that contains two 12-AWG conductors (one for a single phase and the other for the neutral terminal connection), as shown in Figure 2. The geometrical elements shown in Figure 2 are related, for primary parameter calculation purposes, as follows:

**a:** conductor radius

**d:** distance between the centers of the two inner conductors. For the purposes of this study an approximate value of  $d = 1.20584 \cdot 2 \cdot a$  was considered. This particular value was assumed since the average separation between conductors within pipelines is 3mm.

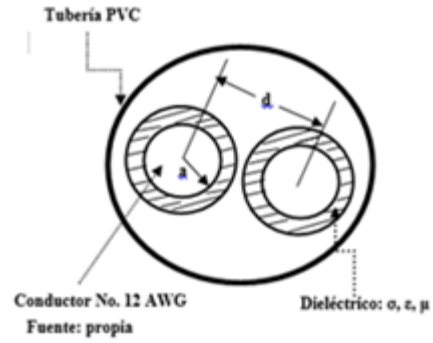


**Figure 2:** geometrical elements

Referring back to Figure 1, it is worth mentioning that the impedance units for  $Z_1$  and  $Z_2$  are Ohms ( $\Omega$ ). However, for the case of conductors, impedances result from conductor length, thus the previous impedances associated to transmission lines were given as  $Z'1(\Omega/m)$  and  $Z'2(\Omega/m)$ .

$$Z = Z'(\Omega / m) \cdot longitud (m); (\Omega) \quad (5)$$

Similarly, the units of admittance  $Y$  are Mhos or Siemens ( $\sigma$ ) and are associated to the line's length as follows:  $Y'(\sigma/m)$

$$Y = Y'(\text{siemens} / m) \cdot length (m); (\text{siemens}) \quad (6)$$

Each of the elements that contribute to the impedance and admittance, are presented as follows:

$$Z = R' \cdot \Delta x + j\omega L' \cdot \Delta x; (\Omega) \quad (7)$$

$$Y = G' \cdot \Delta x + j\omega C' \cdot \Delta x; (\text{siemens}) \quad (8)$$

In this description,  $R'$  represents resistance,  $a$  is the conductor radius,  $\sigma$  is conductivity and  $\delta$  represents the skin depth factor of equation 2.

$$R' = \frac{\sqrt{f}}{(\pi \cdot a \cdot \sigma \cdot \delta)}; (\Omega / m) \quad (9)$$

The expression for inductance  $L'$  is as follows:

$$L' = \frac{\mu}{(\pi \cdot)} \cdot \text{Cosh}^{-1}\left(\frac{d}{2 \cdot a}\right); (F / m) \quad (10)$$

Where  $a$  is the conductor radius,  $\mu$  is the permeability constant and  $d$  represents the separation distance between conductors. The expression for capacitive loss  $C'$  is:

$$C' = \frac{\pi \cdot \epsilon}{\text{Cosh}^{-1}\left(\frac{d}{2a}\right)}; (H / m) \quad (11)$$

Where  $\epsilon$  represents the permittivity constant. The expression for conductance  $G'$  is as follows:

$$G' = 2\pi \cdot f \cdot C' \cdot \tan \delta; (\text{simens} / m) \quad (12)$$

In this expression  $C'$  is computed from (11) and  $\tan \delta$  represents the skin-depth loss factor indicated in equation (2). Once all the main parameters of the transmission line are calculated, the results are multiplied by the corresponding length and frequencies so that they can be represented as indicated in equations (7) and (8).

$$Z = R + jX = N \quad \phi \quad (13)$$

After obtaining the values of  $Z$  and  $Y$  from equations (9) to (12), to be used in equations (7) and (8), and since each element of the transmission line matches these equations, from Figure 1 we can obtain a complex-valued representation (either rectangular or polar) for  $Z$  and  $Y$  as follows:

$$Y = G + jB = N \quad \phi \quad (14)$$

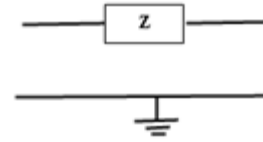
Where  $X = \omega L$  ( $\Omega$ ) and  $B = \omega C$  (siemens), respectively. Then, applying the quadripole model and the transmission parameters that allow a matrix-form manipulation for complex variables, it is possible to achieve operation results that are efficient in terms of transfer functions (vector length  $N$  and angle  $\phi$ ), input/output impedances, and voltage/current gains, among other resulting values. The model has the following representation:

$$\begin{pmatrix} V_i \\ I_i \end{pmatrix} = \begin{pmatrix} a_{11} & a_{12} \\ a_{21} & a_{22} \end{pmatrix} \begin{pmatrix} V_o \\ I_o \end{pmatrix} \quad (15)$$

Where  $V_i$ ,  $I_i$ , and  $V_o$ ,  $I_o$  correspond to the input and output variables of the quadripole, respectively, and the entries  $a_{ij}$  characterize the transmission matrix.

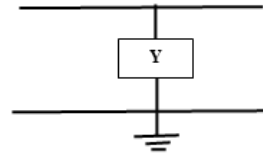
$$\begin{pmatrix} a \\ \mathbf{a} \end{pmatrix} = \begin{pmatrix} a_{11} & a_{12} \\ a_{21} & a_{22} \end{pmatrix} \quad (16)$$

The modeling of each of the line's elements as an independent quadripole suggests the following matrix representation for impedance ( $Z$ ) and admittance ( $Y$ ), so called transmission matrix  $[a]$ :



$$\begin{pmatrix} a \\ \mathbf{a} \end{pmatrix} = \begin{pmatrix} 1 & Z \\ 0 & 1 \end{pmatrix}$$

Figure 3. Impedance



$$\begin{pmatrix} a \\ \mathbf{a} \end{pmatrix} = \begin{pmatrix} 1 & 0 \\ Y & 1 \end{pmatrix}$$

Figure 4. Admittance

The resulting transmission matrix for the network of Figure 1 is as follows:

This matrix is transformed into the following matrix after making some necessary computations:

$$\begin{pmatrix} a \\ \mathbf{a} \end{pmatrix} = \begin{pmatrix} 1 & Z_1 \\ 0 & 1 \end{pmatrix} \begin{pmatrix} 1 & 0 \\ Y_2 & 1 \end{pmatrix} \begin{pmatrix} 1 & Z_3 \\ 0 & 1 \end{pmatrix} \quad (17)$$

$$\begin{pmatrix} a \\ \mathbf{a} \end{pmatrix} = \begin{pmatrix} 1 + Z_1 \cdot Y_2 & Z_3 + Z_1(1 + Y_2 \cdot Z_3) \\ Y_2 & 1 + Y_2 \cdot Z_3 \end{pmatrix} \quad (18)$$

By associating the previous matrix to the matrix in equation (16), the following parameters are obtained:

$$a_{11} = 1 + Z_1 \cdot Y_2 \quad (19)$$

$$a_{12} = Z_3 + Z_1(1 + Y_2 \cdot Z_3) \quad (20)$$

$$a_{21} = Y_2 \quad (21)$$

$$a_{22} = 1 + Y_2 \cdot Z_3 \quad (22)$$

Proceeding with the previous parameters, we obtain the following:

$$H(f) = \frac{V_2}{V_1} = \frac{1}{a_{11}} = \frac{1}{1 + Z_1 \cdot Y_2} \quad (23)$$

This equation corresponds to the transfer function of the transmission line under consideration.

### APPLICATIONS

For a particular design method for in-between-node filters derived from a single phase topology and also by using the results from the transfer function, the characteristics of the filter can be modeled and controlled since these characteristics and the corresponding transfer function are closely related. This procedure is to be carried out in between various pairs of nodes with variations in conductor length (cables and/or wires) and operation frequency (ranging from 1.8 MHz to 30 MHz).

Once filter characteristics have been established, filter behavior can be assimilated from an out-of-filter perspective by implementing electronic designs that exhibit the same frequency response.

Power spectral density [7] is a parameter that allows reducing the impacts of electromagnetic compatibility (noise, attenuation, distortion, coupling) [8]-[9]-[10]-[14] on a particular BPL communications channel [15]-[18] and also facilitates control management over transmission power levels. In general, this type of filter design contributes to properly controlling and reducing electromagnetic compatibility issues as well as taking advantage of transmission power.

### PRELIMINARY RESULTS

Based on measurements obtained from an actual single-phase topology of a household BPL system, adjustments and corrections must be made for a particular set of modeled filters, which have been designed and implemented, to establish response patterns according to circuit location within the topology and also to establish frequency response and transmission SNR levels.

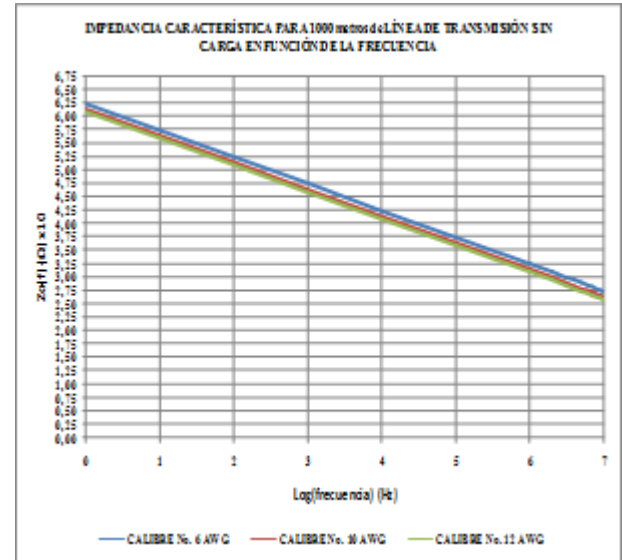
In order to obtain preliminary results for the case of non-loaded 12-AWG conductors within PVC pipelines – galvanic metallic conduit –, a draft algorithm design was carried out using a spreadsheet so as to allow controlling the transmission line based on the line's characteristic impedance and its transfer function. Frequency variations were applied (1.8 MHz and 30 MHz) and conductor length was also varied (between 0.5 and 1000 meters).

### PRELIMINARY RESULTS DISCUSSION

A primary parameter that allows analyzing the behavior of a transmission line (in terms of frequency and line-length variations) that is associated to a single-phase topology is the characteristic impedance  $Z_0$ . Graph 1 shows the results of preliminary calculations that were obtained from the two-conductor configuration of Figure 2 (characteristic impedance described in equation 24 for certain frequency

range variations and for different conductor-gauge computations based on equations 7, 8 and 23).

Graph 1



Graph 1 shows a decreasing variation of the 1000-meter line's characteristic impedance as a function of frequency, which corresponds to an approximate attenuation value of 6 Ω per decade, that is (for the wire gauges under consideration), the non-loaded transmission line exhibits a 6-Ω reduction as the frequency increases by a factor of 10.

$$Z_0 = \sqrt{\frac{(R' + j\omega L')}{(G' + j\omega C')}} \quad (24)$$

For 1 MHz, the following values were obtained:  
 $Z_0(6 \text{ AWG}) = 57,5 \Omega$ ;  $Z_0(10 \text{ AWG}) = 55,5 \Omega$ ;  $Z_0(12 \text{ AWG}) = 54 \Omega$ .

For 30 MHz, the following values were obtained:  $Z_0(6 \text{ AWG}) = 27,5 \Omega$ ;  $Z_0(10 \text{ AWG}) = 26,5 \Omega$ ;  $Z_0(12 \text{ AWG}) = 25 \Omega$ .

For illustration purposes it is worth mentioning that a 60-Watt load (standard lighting output) that operates at 110 Volts and 60 Hz has an impedance of 202 Ω. In the case of a 1000-Watt load (e.g. irons or electric drills), impedance values are about 12 Ω. The characteristic impedance of a transmission line for a single-phase topology is capable of dealing with load variations, as illustrated in the following sections.

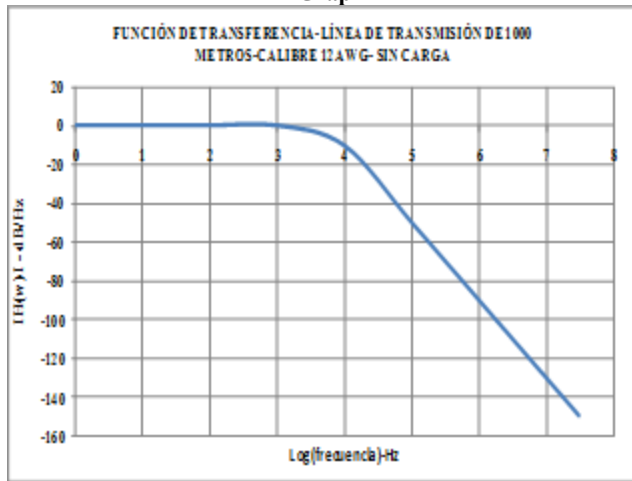
A typical equation of a transfer function (equation 23) ensures a filter-like behavior of the non-loaded transmission line, within a single-phase topology, when facing frequency or line-length variations. Initially, various calculations and the corresponding analysis were carried out based on the particular transfer function in order to determine the type of filter that can be obtained when varying operation frequency from 1.8 MHz to 30 MHz. Subsequently, a similar procedure was followed

regarding line-length variations ranging from 0.5 m to 1000 m.

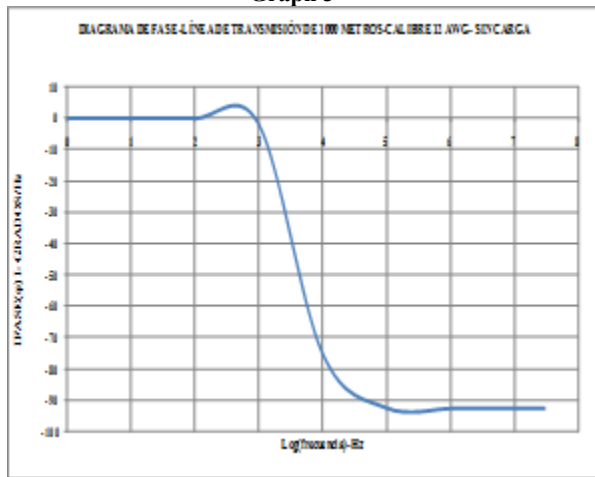
It is worth mentioning that the algorithm employed yields results in terms of both magnitude and phase, which represent characteristic variables for the filters in question.

**Frequency response of the transfer functions.** The aforementioned methodology was developed until finding a final version of a computation algorithm that allowed obtaining suitable results from equation 21, particularly when varying the operation frequency for transmission-line lengths of around 1000 meters. The results in terms of both magnitude and phase are shown in Graphs 2 and 3, respectively.

**Graph 2**



**Graph 3**



Graph 2 indicates that, in terms of frequency response, line behavior for a 12-AWG-conductor transmission line corresponds to a second-order low-pass filter, provided its 40-dB per decade decreasing slope [20]. This suggests that the transmission line in question offers an attenuation of -40 dB (when comparing output signals with transmitted input signals) as operation frequency increases by a factor of 10. The dotted line represents the values for which an attenuation of -3 dB can be obtained, which corresponds to

a cutoff frequency of about 10000 Hz (a point in frequency at which output signal power is half of the transmitted signal power). For frequency values over 10000 Hz, output power is attenuated by 40 dB per decade. Regarding phase behavior, there is a phase shift of  $-90^\circ$  per decade, that is, there is a phase variation between the input and output signal of  $-90^\circ$ , and, as frequency increases, there is a non-loaded line behavior that resembles an inductive response.

In general, one of the goals of the present study is to find a method to control the shift in cutoff frequency values at frequencies over 10000 Hz, whether the BPL transmission line associated to a single phase topology is loaded or not; thus it is ensured that transmission power passes over a larger bandwidth. Figure 5 shows the results of the algorithm for operation frequencies of around 30 MHz and 1000-meter line length.

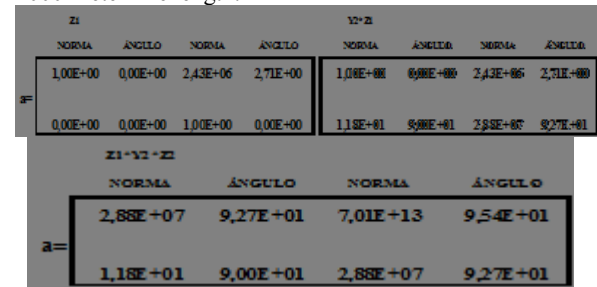


**Figure 5:** Results of the algorithm

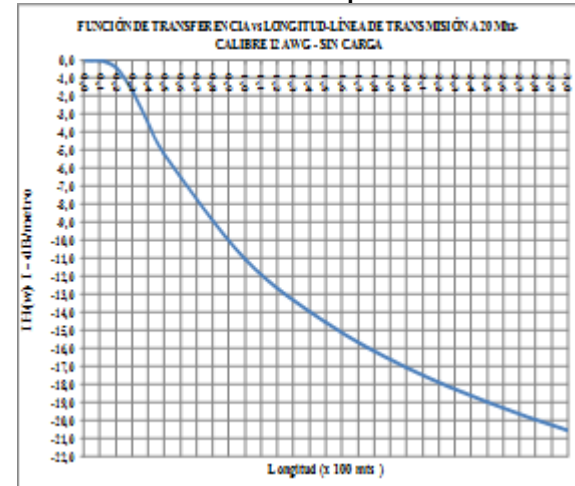
Figure 6 shows the algorithm's control capabilities in terms of input/output performance.

CONTROL DE ENTRADA/SALIDA DEL ALGORITMO		
(FRECUENCIA CONSIDERADA) f=	30000000	Hz
LONGITUD CONSIDERADA=	1000	metros
FUNCIÓN DE TRANSFERENCIA	NORMA	ÁNGULO
V2/V1= H(w) = a	3.4688E-08	-92.713

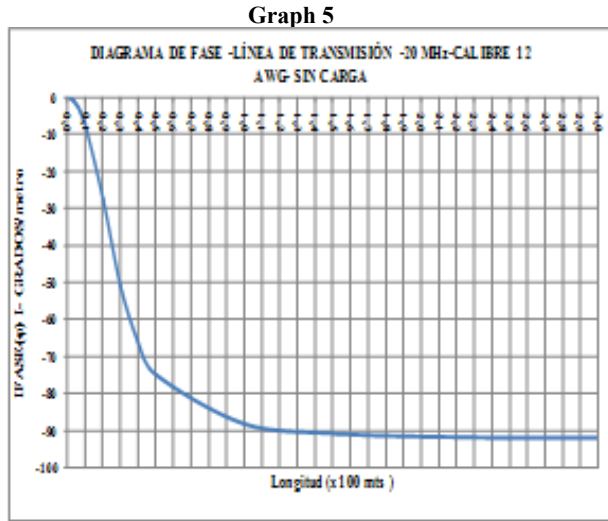
**Figure 6:** Algorithm's control

**Line-length response of the transfer function.** By using the same computation algorithm on equation 21, transmission line length was varied for an operation frequency of 20 MHz. The results in terms of magnitude and phase are shown in Graphs 4 and 5, respectively.

**Graph 4**



Graph 4 illustrates the behavior of the transmission line for a 12-AWG conductor regarding length variations. This corresponds to a low-pass filter with a -10-dB per decade slope as a function of length. This suggests that the transmission line offers an attenuation of -10 dB (comparing output signals to input signals) as length increases by a factor of 10. The dotted line shows the point at which attenuation of -3 dB occurs. This point corresponds to a cutoff length of 40 meters, thus for such length and an operation frequency of 20 MHz, the output signal power is half that of the transmitted power. For values over 40 meters, the output power is attenuated by 10 dB per decade of length.



In Graph 5, it can be seen that, for the 12-AWG-conductor transmission line, regarding length variations, there is a phase-shift behavior of  $-90^\circ$  every 100 meters, there is a phase variation between input signal and output signal of  $-90^\circ$ . The overall behavior of non-loaded transmission line, as a function of length, is inductive.

It is necessary to determine a method to control the point at which the cutoff length occurs for values over 40 meters and a transmission line associated to a BPL single-phase topology (whether loaded or not). This ensures that the transmitted power flows over a larger bandwidth.

#### OBSERVATIONS ON LOADED TRANSMISSION LINES

Referring to Figure 1, when a particular load ( $Z_L$ ) is added, in parallel, to the circuit's output, the network shown in Figure 7 is obtained.

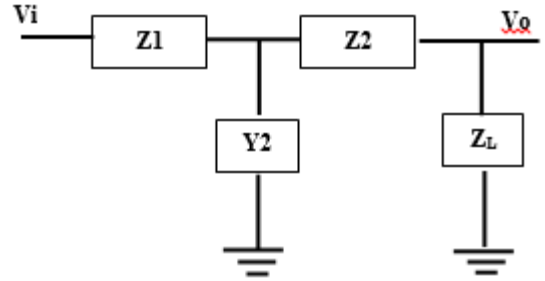


Figure 7: Network obtained

Since the power transmission line is going to be used as a BPL communications channel, and as observed in section 2.1 and Graph 2, there is an attenuation of -3 dB at a cutoff frequency equal to 10 KHz. The purpose of placing a particular load at the output terminal of the transmission line is to establish the characteristics of such a load that permit finding an upper cutoff frequency of 10 KHz so as to ensure efficient power transmission.

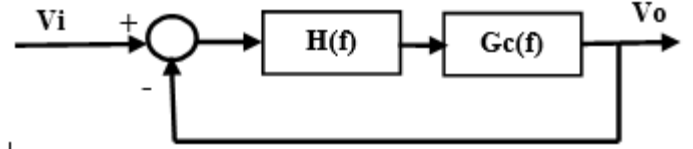


Figure 8

The phase diagram of Graph 3 indicates that there is an inductive behavior of the transfer function associated to equation 21, which suggests that the transfer function should be *compensated* [21], [22], [23] by using a capacitive load.

An important aspect that should be considered when loading the transmission line involves choosing the values for the components that are to constitute the *compensator*. These components must ensure a larger frequency response (Figure 8 illustrates this situation). The feedback loop that appears in the diagram ensures that there is no further (sharper) attenuation at the output. Since a particular load might be represented as certain admittance value, the following can be obtained:

$$Y_L = \frac{1}{Z_L} = G_L * k_1 * \Delta x + j\omega C_L * k_2 * \Delta x \quad (25)$$

In equation 25, constants  $k_1$  and  $k_2$  correspond to a pair of values that affect the behavior of the compensator and so, by using the feedback loop such values are adjusted, yielding the following (equation 26):

$$k_1 = \frac{R_L}{R_2} = \frac{G_2}{G_L}, k_2 = \frac{C_2}{C_L} \quad (26)$$

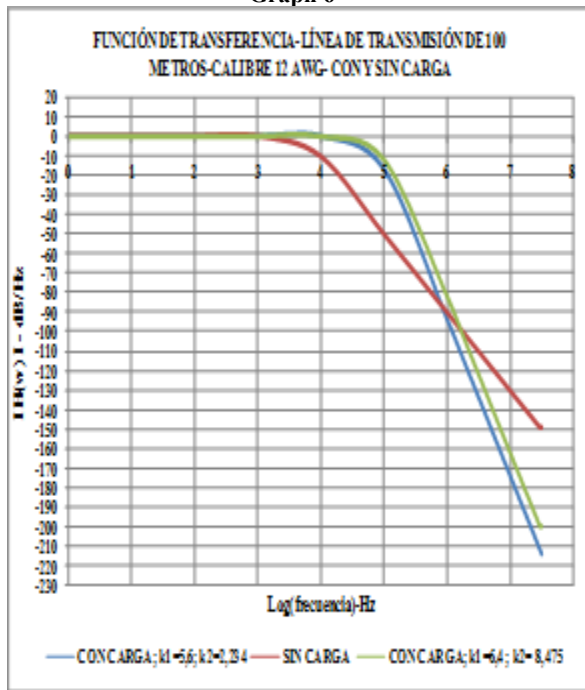
It is necessary to express the elements of the load impedance as a function of the line's admittance elements, thus frequency and length compensation is guaranteed. The network section displayed in Figure 7, which corresponds to  $Z_L$ , was modeled according to Figure 4, and it was used within the transmission-parameter model to subsequently run the computation algorithm.

The assessment of  $k_1$  and  $k_2$  for two different types of load impedance can be summarized by the data shown in Table 12.

Table No. 12

$k_1$	$k_2$	1 Hz RL( $\Omega$ )	30 MHz RL( $\Omega$ )	1 Hz CL( $\mu$ F)	30 MHz CL( $\mu$ F)
5,6	2,234	1,65611,8168	3,95711E-07	0,002812397	0,002812395
6,4	8,475	1,86784,9335	1,13796E-06	0,000741345	0,000741344

Graph 6

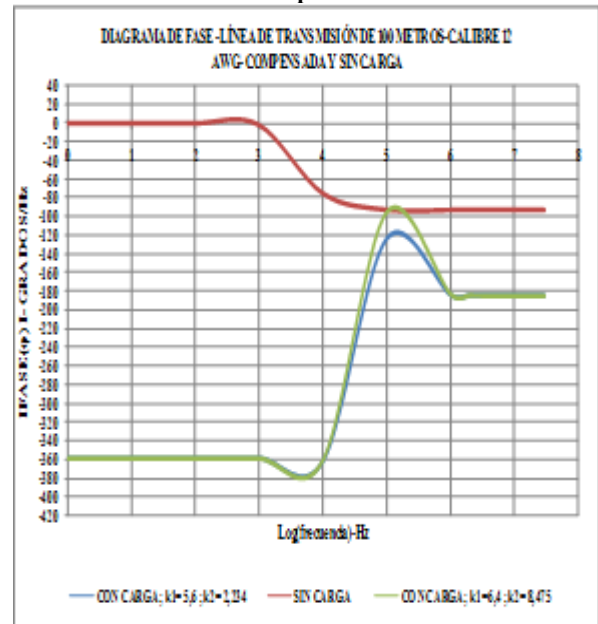


The results obtained for the transfer function and the phase diagram appear in Graphs 6 and 7, respectively.

Graph 6 shows the behavior of a compensated (and loaded) transmission line for a 12-AWG conductor as a function of frequency. It can be observed that the line exhibits the characteristics of a third-order low-pass filter due to its -60 dB per-decade decreasing slope. This indicates that the transmission line in question offers attenuation of -60 dB (when comparing output signals to input signals) whenever operation frequency increases by a factor of 10. The dotted line indicates the frequency value for a -3 dB attenuation, which corresponds to a cutoff frequency of 100000 Hz, that is, at this particular frequency, the power of the output signal is half the power of the transmitted signal. For frequency values over

100000 Hz, output power is attenuated by 60 dB per frequency decade. By applying the compensator, a bandwidth gain of 10 was achieved.

Graph 7



In Graph 7, it can be observed that there is a phase forward shift that ranges from  $-380^\circ$  to  $-120^\circ$  and also to  $-100^\circ$  per decade, respectively for the two load conditions illustrated in Table 12. This means that the compensator produced phase variations between the input and output signals of approximately  $-250^\circ$ , and the overall behavior of the compensated (and loaded) transmission line is mostly capacitive as a function of frequency. Complete verification of the line's operation is achieved by implementing line-length variations. To this end, the same *compensator-wise* scheme (Figure 8) was applied using the same restrictions on the values of  $k_1$  and  $k_2$  (see equations 23 and 24) as well as considering an operation frequency of 20 MHz. The results regarding magnitude and phase are shown in Table 13, and Graphs 8 and 9, respectively.

Table 6

$k_1$	$k_2$	1 metro RL( $\Omega$ )	300 metros RL( $\Omega$ )	1 metro CL( $\mu$ F)	300 metros CL( $\mu$ F)
5,6	2,234	0,018292373	1,829237E-05	2,81239E-07	0,000281239
6,4	8,475	0,018292373	1,829237E-05	2,81239E-07	0,000281239

signals to input signals) whenever there is an increase in length by a factor of 10. After including the compensator, there was virtually no bandwidth gain, and if any such gain were to be observed, it would be negligible.

Graph 9 shows that there is a forward phase shift ranging from  $-440^\circ$  to  $-180^\circ$  per decade, respectively for the load conditions illustrated in Table 13. This indicates that the compensator yielded a phase variation, between the output and input signals, of approximately  $-260^\circ$ ; and the overall behavior of the compensated (and loaded) transmission line is mostly capacitive as a function of frequency.

### CONCLUSIONS

The behavior of a 12-AWG-conductor transmission line associated to a single-phase BPL household topology resembles that of a low-pass filter (whether loaded or not). The transfer-function frequency response for the non-loaded transmission line corresponds to a second-order filter whose slope decreases at  $-40$  dB per decade as a function of frequency. This means that the transmission line offers attenuation of  $-40$  dB as the frequency increases by a factor of 10, with a cutoff frequency of 10000 Hz.

In the case of non-loaded transmission lines, the phase shift corresponds to a slope of  $-90^\circ$  per decade. The overall behavior as a function of frequency is mostly inductive.

The behavior of the non-loaded 12-AWG-conductor transmission line as a function of the line's length, at an operation frequency of 20 MHz, resembles that of a low-pass filter. The slope of such a filter is  $-10$  dB per length decade; in other words, the transmission line offers attenuation of  $-10$  dB as its length increases by a factor of 10. The cutoff length for the filter is 40 meters; therefore for values over 40 meters, the output power is reduced by 10 dB per length decade.

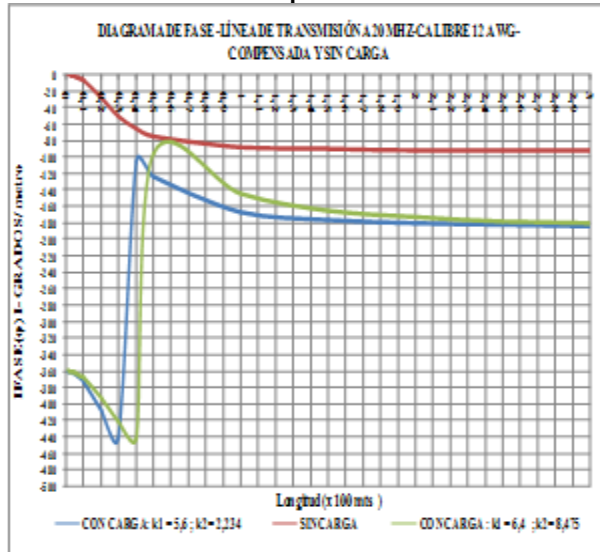
Regarding the phase shift of the 12-AWG-conductor transmission line as a function of length, the overall behavior suggests a  $-90^\circ$  phase shift every 100 meters; and the non-loaded line's behavior is mostly inductive as a function of length.

The behavior of the compensated (and loaded) 12-AWG transmission line, as a function of frequency, resembles that of a third-order low-pass filter whose slope corresponds to  $-60$  dB per decade. Thus the transmission line offers attenuation of  $-60$  dB after increasing the operation frequency by a factor of 10. The cutoff frequency in this case was 100000 Hz.

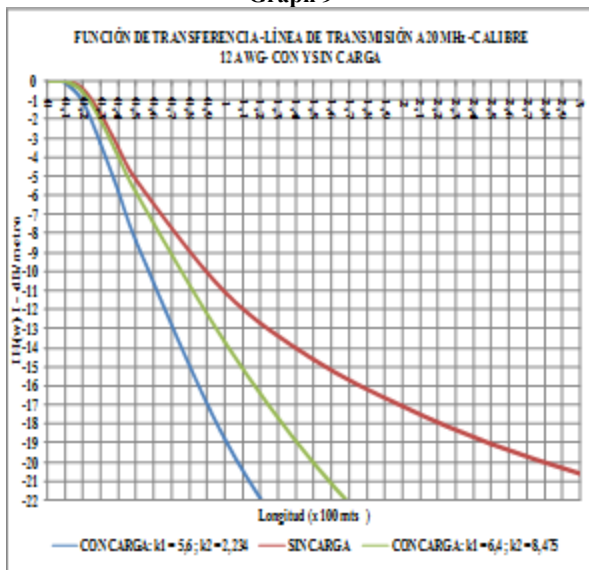
In the case of the loaded transmission line, there was a forward phase shift ranging from  $-380^\circ$  to  $-120^\circ$  and also to  $-100^\circ$  per decade, respectively. The compensator that was implemented yielded a phase-shift variation (between the input and output signals) of  $-250^\circ$ , and the overall behavior of the compensated (and loaded) transmission line is mostly capacitive as a function of frequency.

The behavior of the compensated (and loaded) 12-AWG transmission line as a function of length resembles that of a first-order low-pass filter. The slope of such a filter is  $-20$  dB per frequency decade. The transmission line offers attenuation of  $-20$  dB as the line length increases by a factor of 10. After implementing the compensator, there was no bandwidth gain; in case this bandwidth gain was to

Graph 8



Graph 9



In Table 13, it can be observed that, for the same length variations, the compensator-associated values of  $k_1$  and  $k_2$  take the same border values for both the resistance load and capacitance load. Graph 8 shows that the overall behavior of compensated (and loaded) transmission line for a 12-AWG conductor, as a function of length, resembles that of a first-order low-pass filter, as it can be observed by looking at the  $-20$  dB per-decade decreasing slope. This indicates that the transmission line in question offers attenuation of  $-20$  dB (when comparing output

be achieved, it would be negligible. Regarding the signal's phase, there was a forward phase shift ranging from  $-440^\circ$  to  $-180^\circ$  per decade, respectively. The compensator yielded a comparative variation, between input and output signals, of approximately  $-260^\circ$ , and the overall behavior of the compensated (and loaded) line as a function of frequency is mostly capacitive.

The frequency response of the low-pass filter associated to the transfer function of the loaded transmission line shows better results than the non-loaded line in terms of bandwidth.

The length-dependent response of the low-pass filter associated to the transfer function of the loaded transmission line shows limited results in terms of bandwidth when compared to the bandwidth of the non-loaded transmission line.

## REFERENCES

- [1] García, G; Estopiñán, A.; García, M. Circuitos de parámetros distribuidos: Aplicación a líneas de transporte de energía eléctrica. 1. ed. España. Prensas de la Universidad de Zaragoza.1996. 206 p. ISBN 8477334668 ISBN-13 9788477334668
- [2] Bastidas H.; Patiño, M. ; Ángel, G. Modelo de cálculo de los parámetros técnicos de las líneas eléctricas de baja tensión subterráneas e instalaciones internas para uso en telecomunicaciones. Universidad Nacional. *Revista: Ingeniería e investigación vol. 31 No. 3, diciembre 2011 (121-129)*.
- [3] Scott, D. Análisis de Circuitos Eléctricos. 1 ed. España. Editorial McGraw-Hill. 1988.720p. ISBN: 84-7615-269-8..
- [4] Cárdenas, R. Red Residencial de Banda Ancha por Línea de Potencia Basada en Relevos para la Mitigación de la Interferencia v.2.1. Tesis presentada como requisito parcial para optar al título de Doctor en Ingeniería Eléctrica. Universidad Nacional de Colombia. 2013.
- [5] ICONTEC. Norma Técnica Colombiana. NTC 2050. Código Eléctrico Colombiano. 1998-11-25.
- [6] Carlson, A.B., Sistemas de Comunicación. Mc Graw Hill. 3ªEdición. 2003.
- [7] VINIOTIS, Yanis. Probability and random processes for electrical engineers. 1 ed. New York : Editorial Mc. Graw –Hill, 1998. 676p. ISBN 0-07-067491-4
- [8] Blackman CF, Benane SG, House DE. The influence of 1.2 microT, 60 Hz magnetic fields on melatonin- and tamoxifen-induced inhibition of MCF-7 cell growth. *Bioelectromagnetics* 2001; 22:122-128.
- [9] Zimmermann & Doster, A Multi-Path Signal Propagation Model for the Power Line Channel in the High Frequency Range, 1999) (Zimmermann & Dostert, A Multipath Model for the Powerline Channel, 2002)
- [10] E. M. Purcell, *Berkeley physics course, volumen 2, Electricidad y Magnetismo* (Reverté, Barcelona, 1969).
- [11] Galli, S. Power line communications. IEEE Communication Theory Workshop, Cancun,2010.
- [12] Couch II, León W., Sistemas de Comunicaciones Digitales y Analógicos. Prentice Hall, Quinta Edición, México, 2004.
- [13] Dorf, S., Circuitos Eléctricos Introducción al Análisis y Diseño., Alfaomega editores. 5ª Edición, México, D.F., 2007
- [14] Dostert, K., Zimmermann, M., Waldeck, T., Arzberger, M., Fundamental properties of the low voltage power distribution grid used as a data channel., *European Transactions on Telecommunications (ETT)*, Vol. 11, No. 3, May/June 2000.
- [15] Dostert, K., Telecommunications over the power distribution grid possibilities and limitations., *Proceedings of the 1997 International Symposium on Power Line communications and Its Applications*, Essen, Germany, April 1997.
- [16] Instituto Colombiano de Energía Eléctrica - ICEL., Normas para el diseño y construcción de sistemas de subtransmisión y distribución, Volumen IV – 1998
- [17] Instituto Colombiano De Normas Técnicas Y Certificación- ICONTEC., Reglamento Técnico de Instalaciones Eléctricas- RETIE, 2007.
- [18] Dostert, K., Zimmermann, M., Waldeck, T., Arzberger, M., Fundamental properties of the low voltage power distribution grid used as a data channel., *European Transactions on Telecommunications (ETT)*, Vol. 11, No. 3, May/June 2000.
- [19] International Telephone and Telegraph Co., Inc: "Reference Data for Radio Engineers". 5 ed. Howard W. Sams and Co. Indianapolis, Ind. 1968.
- [20] Boylestad R., Electrónica teoría de circuitos. 5 ed. México. 1994. 913 p. ISBN 968-880-347-2.
- [21] Ogata K., Ingeniería de control moderna. 3 ed. México. 1998. 997 p. ISBN 0-13-227307-1.
- [22] FACTS Controllers to Improve Voltage Profile and Enhancement of Line Loadability in EHV Long Transmission Lines Shankaralingappa C. B, and Suresh. H. Jangamashetti, Senior member, IEEE. 2013.
- [23] Fault component integrated impedance-based pilot protection scheme for the TCSC compensated EHV/UHV transmission line HE ShiEn1, 2\*, SUONAN JaLe1 & KANG XiaoNing